Solid State Ionics 275 (2015) 19–22

Contents lists available at ScienceDirect

Solid State Ionics

journal homepage: www.elsevier.com/locate/ssi

Proton conduction at BaO-terminated (001) $BaZrO_3$ surface using density functional theory

Ji-Su Kim [a], Jin-Hoon Yang [a], Byung-Kook Kim [b], Yeong-Cheol Kim [a,*]

[a] School of Energy, Materials, and Chemical Engineering, Korea University of Technology and Education, Cheonan 330-708, Republic of Korea
[b] High Temperature Energy Materials Research Center, Korea Institute of Science and Technology, Seoul 136-791, Republic of Korea

ARTICLE INFO

Article history:
Received 17 October 2014
Received in revised form 18 February 2015
Accepted 12 March 2015
Available online 3 April 2015

Keywords:
Proton conduction
Computer simulation
Surface
Space charge layer
Structural disorder

ABSTRACT

We studied proton conduction at a BaO-terminated (001) $BaZrO_3$ surface by using density functional theory. In order to evaluate the proton conductivity at the surface, the space charge layer and structural disorder models were introduced. In the BaO-terminated (001) $BaZrO_3$ surface, a positively-charged proton and an oxygen vacancy were segregated at the surface layer with segregation energies of −0.96 and −0.42 eV, respectively; this results in the generation of the Schottky barrier height. The migration energy barrier of the proton at the surface was 1.03 eV, and was converted to the proton mobility at the surface. Based on the concentration and mobility of the proton, its conductivity at the surface was evaluated. We find that the surface impedes the proton conduction by six orders of magnitude more than bulk at 900 K.

1. Introduction

Since Iwahara introduced strontium zirconate and strontium cerate as proton-conducting ceramic electrolytes in early 1980s, many researchers have worked on perovskite materials [1,2]. Among those perovskite materials, barium zirconate ($BaZrO_3$) is one of the appropriate intermediate temperature proton-conducting electrolytes for protonic ceramic fuel cells (PCFCs) due to its stability and high proton conductivity in bulk [3–10]. $BaZrO_3$, however, shows low conductivity at grain boundaries, and much research has been devoted to understand its origin; the low proton conductivity at grain boundaries has been interpreted by using the space charge layer and structural disorder models [11–17].

Contrary to the studies of proton conduction at grains and grain boundaries, the proton conduction at surfaces has not been widely investigated yet. Since all the protons should conduct through surfaces before or after conducting through grains and grain boundaries for PCFCs, the proton conduction at surfaces is essential to understand the overall proton conduction in PCFCs. To evaluate the proton conduction at a surface, the most stable surface should be analyzed first. Ho et al. investigated the stability of the (001) $BaZrO_3$ surface using density functional theory (DFT), and mentioned that the BaO-terminated (001) $BaZrO_3$ surface was stable [18]. Heifets et al. investigated the stability of the (001) and (011) $BaZrO_3$ surfaces using DFT, and mentioned that the BaO-terminated (001) $BaZrO_3$ surface was the most stable among the nine tested surfaces [19]. Calleja et al. investigated $BaZrO_3$ nanoparticles fabricated by electrospinning method using transmission electron microscopy, and mentioned that the $BaZrO_3$ nanoparticles were cubic-like with (001) surfaces [20].

In this work, we investigated the proton conduction at the BaO-terminated (001) $BaZrO_3$ surface by using DFT. In order to understand the proton conduction at the surface, the concentration and mobility were calculated based on the space charge layer and structural disorder models. Based on the two models, the proton conductivity at the surface was evaluated, and compared with those of bulk and grain boundaries.

2. Calculation details

All calculations were performed using the Vienna ab-initio simulation package (VASP) based on DFT [21–24]. Electron wave functions were described using the projector augmented wave (PAW) method of Blöchl implemented in the VASP by Kresse and Joubert [25,26]. The exchange correlation energy was described by the generalized gradient approximation (GGA) of Perdew, Burke, and Ernzerhof (PBE) [27]. The wave functions were expanded in plane waves with a cutoff energy of 500 eV. Partial wave occupancies were calculated with the Gaussian smearing method, and the width of smearing was 0.05 eV. Electronic and geometric optimizations were converged when the total energy difference between successive calculation steps was less than 10^{-3} and 10^{-2} eV, respectively. All atoms were allowed to relax until the force on each atom was below 0.005 eV/nm.

* Corresponding author at: 1600 Chungjeollo, Byeongcheon-Myeon, Cheonan, Chungnam 330-708, Republic of Korea. Tel.: +82 41 560 1326; fax: +82 41 560 1360.
E-mail address: yckim@koreatech.ac.kr (Y.-C. Kim).

http://dx.doi.org/10.1016/j.ssi.2015.03.021
0167-2738/

Using these computational settings, the $BaZrO_3$ unit cell was optimized with an 8 × 8 × 8 *Monkhorst–Pack* *k*-points mesh [28], and the calculated lattice parameter of 0.425 nm was in good agreement with the experimentally-measured (0.419 nm) and theoretically-calculated (0.425 nm) results within 1.4% error [5,13,29]. A 2 × 2 BaO-terminated (001) $BaZrO_3$ surface structure with 14 layers and 1.5 nm vacuum on top was constructed using the optimized unit cell with a 4 × 4 × 1 *k*-points mesh, as shown in Fig. 1(a). The 1.5 nm vacuum was large enough to neglect the interaction between the two surfaces of the surface structure. The bottom two layers were fixed, while the top 12 layers were allowed to relax. The proton migration energy barriers at the surface structure were calculated using the climbing nudged elastic band (CI-NEB) tool [30]. All images were drawn using the Visualization for Electronic and Structural Analysis (VESTA) tool [31].

The space charge layer model was introduced to calculate the electrostatic potential difference at the surface and concentrations of proton and doubly positively charged oxygen vacancy [12–16,32,33]. The Mott–Schottky approximation is assumed for a constant dopant concentration throughout the material to surface. The trivalent dopant concentration, the partial pressure of water, and the relative dielectric constant were set to 10%, 0.025 atm, and 46 [7], respectively. The hydration enthalpy and entropy of $BaZrO_3$ were −0.79 eV and −0.89 meV/K, respectively [3]. More details of the space charge layer model are explained in refs. [12–16,32,33].

3. Results and discussion

Fig. 1(b) and (c) shows the energy (E) of the surface structure as a function of the defect (D = proton (H) or oxygen vacancy (V)) position from the surface (z) when a D is inserted into the surface structure. The total number of electrons is varied during the generation of the defect to maintain the charge state of each defect. The segregation energy of defect ($E_{D,seg}$) in the surface structure is calculated as

$$E_{D,seg} = E_D^S - E_D^B$$

where E_D^S is the energy of the surface structure with a D at the surface, and E_D^B is the energy of the surface structure with a D at bulk, which is calculated by averaging the energy values of the surface structure, when a D is positioned away from the surface. E_D^B is set to zero as referenced in E of Fig. 1(b) and (c). The proton energy variation agreed well with the results of Tauer et al. [34]. $E_{H,seg}$ and $E_{V,seg}$ were −0.96 and −0.42 eV, respectively, indicating that the proton had a higher tendency to be segregated than the oxygen vacancy at the surface.

Based on $E_{H,seg}$ and $E_{V,seg}$, the electrostatic potential difference ($\Delta\varphi$) and the concentration of proton or oxygen vacancy (c_D, $D = H$ or V) as a function of z at (a) 600, (b) 900, and (c) 1200 K are calculated by using the space charge layer model [12–16,32,33], as shown in Fig. 2. The #/f.u. in Fig. 2 is the number of the defect per formula unit. The white, dark-yellow, light-yellow, and gray areas represent the vacuum, surface core (*SC*), surface space charge (*SSC*), and bulk (*B*) regions, respectively; surface (*S*) consists of *SC* and *SSC*. The widths of *SC* and *SSC* regions are 0.15 and 1.65 nm at 600 K. $\Delta\varphi(z)$ is expressed as $\Delta\varphi(z) = \varphi(z) - \varphi(\infty)$, where $\varphi(z)$ is the electrostatic potential at z and $\varphi(\infty)$ is that at $z = \infty$ (i.e., bulk); $\Delta\varphi(0)$ is the Schottky barrier height. c_H^{SC} is high while c_V^{SC} is low due to the lower $E_{H,seg}$ (i.e., strong segregation) and the smaller charge state of the proton compared to oxygen vacancy, as shown in Fig. 2(a). $\Delta\varphi(0)$ was 0.83, 0.70, and 0.53 V at 600, 900, and 1200 K, respectively. Due to the high c_H^{SC}, the protons and oxygen vacancies were depleted at the *SSC* region to satisfy the charge neutrality condition, and therefore, $\Delta\varphi(z)$ was exponentially-decreased as a function of z. In contrast to 600 and 900 K, c_V^B was higher than c_H^B at 1200 K due to dehydration at this high temperature.

Fig. 3 shows (a) a proton migration pathway in the surface structure and (b) its migration energy as a function of z. The migration energy barrier (E_m^i, i = *SC*, *SSC*, or *B*) is calculated as

$$E_m^i = E_{TS}^i - E_{initial}^i$$

where E_{TS}^i and $E_{initial}^i$ are the energy at a transition state and an initial state, respectively. E_D^B is set to zero as referenced in E of Fig. 3(b). The calculated E_m^{SSC} was in the range of 0.10–0.28 eV, similar to the calculated undoped E_m^B at $BaZrO_3$ [9,10]. On the other hand, E_m^{SC} was 1.03 eV when the proton migrated from the surface core oxygen to the nearest sub-surface oxygen, which was higher than that at the $\sum 5$ grain boundary (0.68–0.78 eV) [5]. The high E_m^{SC} indicates that the proton

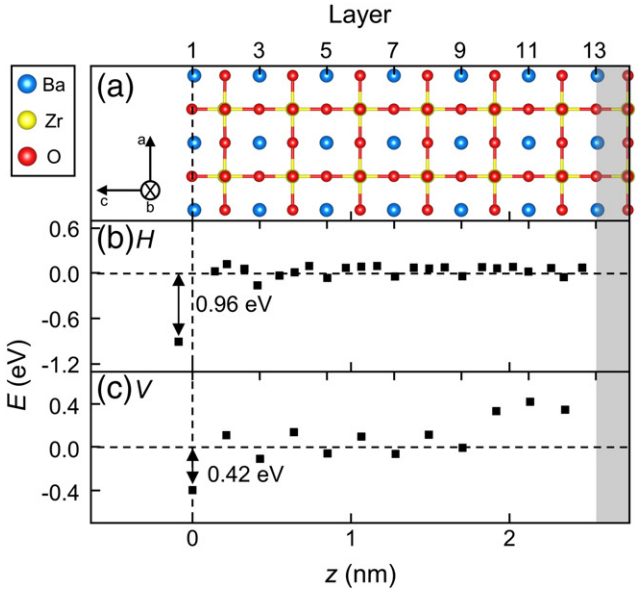

Fig. 1. (a) BaO-terminated (001) $BaZrO_3$ surface with 14 layers and 1.5 nm vacuum on top, shown along the [010] direction, and the energy (E) of the surface structure as a function of the (b) proton (H) or (c) oxygen vacancy (V) position from the surface (z) when a defect ($D = H$ or V) is inserted into the surface structure.

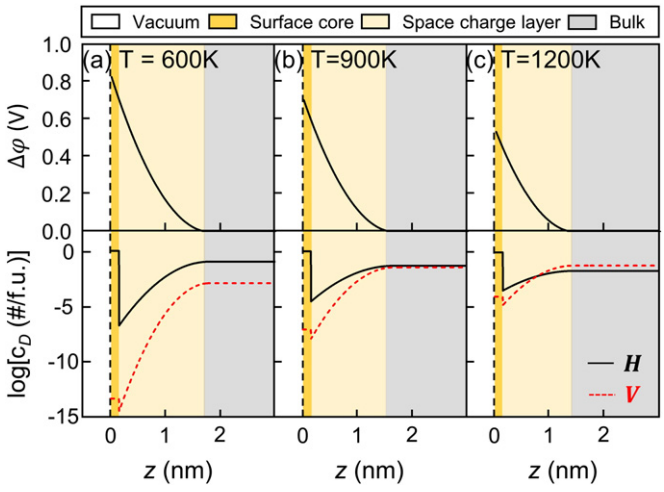

Fig. 2. Profiles of (a) the electrostatic potential difference ($\Delta\varphi$) and (b) the concentrations (C_D) of H and V as a function of z. The white, dark-yellow, light-yellow, and gray areas represent the vacuum, surface core (*SC*), surface space charge (*SSC*), and bulk (*B*) regions, respectively.